Journal of Applied Physics

Growth temperature dependence of Si doping efficiency and compensating deep level defect incorporation in $Al_{0.7}Ga_{0.3}N$

Cite as: J. Appl. Phys. **117**, 185704 (2015); https://doi.org/10.1063/1.4920926
Submitted: 05 February 2015 . Accepted: 25 April 2015 . Published Online: 11 May 2015

Andrew M. Armstrong, Michael W. Moseley, Andrew A. Allerman, Mary H. Crawford, and Jonathan J. Wierer

JOURNAL OF APPLIED PHYSICS **117**, 185704 (2015)

Growth temperature dependence of Si doping efficiency and compensating deep level defect incorporation in $Al_{0.7}Ga_{0.3}N$

Andrew M. Armstrong,[a] Michael W. Moseley, Andrew A. Allerman, Mary H. Crawford, and Jonathan J. Wierer, Jr.
Sandia National Laboratories, Albuquerque, New Mexico 87185, USA

(Received 5 February 2015; accepted 25 April 2015; published online 11 May 2015)

The growth temperature dependence of Si doping efficiency and deep level defect formation was investigated for *n*-type $Al_{0.7}Ga_{0.3}N$. It was observed that dopant compensation was greatly reduced with reduced growth temperature. Deep level optical spectroscopy and lighted capacitance-voltage were used to understand the role of acceptor-like deep level defects on doping efficiency. Deep level defects were observed at 2.34 eV, 3.56 eV, and 4.74 eV below the conduction band minimum. The latter two deep levels were identified as the major compensators because the reduction in their concentrations at reduced growth temperature correlated closely with the concomitant increase in free electron concentration. Possible mechanisms for the strong growth temperature dependence of deep level formation are considered, including thermodynamically driven compensating defect formation that can arise for a semiconductor with very large band gap energy, such as $Al_{0.7}Ga_{0.3}N$.
 [http://dx.doi.org/10.1063/1.4920926]

I. INTRODUCTION

Interest is burgeoning in the potential for Al-rich AlGaN as a semiconductor for the next-generation power electronics applications due to its very large band gap energy (E_g).[1–5] Post-silicon power electronic devices based on GaN and SiC wide band gap semiconductors (E_g of 3.4 eV and 3.2 eV, respectively) are reaching maturity, prompting consideration of "ultra" wide band gap (UWBG) semiconductors such as $Al_xGa_{1-x}N$ ($E_g = 3.4 - 6.2$ eV) for further improvement of power switching performance.[4] Power electronics benefit from larger E_g because the critical electric field scales as $E_g^{2.5}$ for direct band gap semiconductors,[6] so the specific on-resistance scales as $E_g^{-7.5}$.[7] Moreover, very large Schottky barrier energies in excess of 3 eV have been reported for Au/Pt on $Al_{0.5}Ga_{0.5}N$ (Ref. 8) and 4.4 eV for Ni/Au on $Al_{0.81}Ga_{0.19}N$.[2] Such large barriers hold promise for achieving an intrinsically normally off AlGaN-based high electron mobility transistor (HEMT).

Several materials challenges must be overcome before high Al mole fraction $Al_xGa_{1-x}N$ ($x > 0.5$) can utilized in a high performance power transistor. Foremost among these is controlling dopant and defect incorporation. Spontaneous formation of a two dimensional electron gas readily occurs in unintentionally doped AlGaN/GaN HEMTs but has yet to be realized for HEMTs with $Al_xGa_{1-x}N$ channel layers with $x > 0.51$.[3–5] Thus, it appears that control of Al-rich $Al_xGa_{1-x}N$ electrical properties may rely on impurity doping, which is notoriously difficult in UWBG semiconductors.[9]

$Al_xGa_{1-x}N$ becomes very difficult to dope *n*-type for large x.[10,11] For $x > 0.8$, the main challenge to doping is the large thermal ionization energy of the primary donor dopant, Si. Si has been reported to undergo a *DX* transition near $x = 0.8$, and the activation energy of the Si *DX* center increases rapidly for $x > 0.8$ such that only a few percent of the donors are ionized at room temperature.[12] For $Al_xGa_{1-x}N$ $x < 0.8$, Si behaves as a shallow dopant, though strong dopant compensation by deep acceptor-like defects still occurs.[2,10–12] Little is known about deep level defects in $Al_xGa_{1-x}N$ for x approaching 0.8. Achieving a better understanding of the electrical properties of these compensating defect centers and how their incorporation depends on growth conditions will help to identify their physical source and enable more efficient $Al_xGa_{1-x}N$ doping at large x.

This study examined the influence of growth temperature (T_g) on doping efficiency mediated by deep level incorporation in *n*-type $Al_{0.7}Ga_{0.3}N$:Si grown on sapphire by metalorganic vapor phase epitaxy (MOVPE). Growth temperature was considered to be a critical parameter because a T_g-mediated tradeoff was anticipated between morphological and electrical quality in Al-rich AlGaN grown by MOVPE. Higher T_g was expected to improve surface morphology of Al-rich AlGaN epilayers and the sharpness of AlGaN heterointerfaces, based on our observations of improved surface morphology with higher T_g for AlN epilayers grown on sapphire (not shown). However, high T_g could also increase point defect formation and severely compensate dopants in Al-rich AlGaN. AlGaN point defect incorporation at high T_g can be kinetically driven by processes such as Ga desorption from the surface, which leaves behind vacancies. Thermodynamically driven defect formation also become operable at high T_g, where the large E_g of UWBG semiconductors like Al-rich AlGaN can significantly reduce the formation energy (E^f) of compensating defects.[9]

This work used deep level optical spectroscopy (DLOS) and lighted capacitance-voltage (LCV) to quantitatively correlate the T_g-dependence of point defect incorporation and dopant compensation. It was found that the free carrier concentration (n) increased substantially with decreasing T_g.

[a]Electronic mail: aarmstr@sandia.gov.

Reduced compensation by deep acceptors was identified as the mechanism for this trend because an observed decrease in deep level defect concentration (N_t) with lower T_g agreed well with the concomitant increase in n. Carrier compensation was minimal for the lowest T_g used in this study.

II. SAMPLE PREPERATION

The $Al_{0.7}Ga_{0.3}N$ epilayers under study were grown in a Veeco D125 MOCVD at 75 Torr on a 1.5 μm thick AlN layer grown on c-plane sapphire mis-cut 0.15° toward the m-plane. The n-$Al_{0.7}Ga_{0.3}N$ epilayers of interest were grown to 1 μm thickness and doped with Si for a target electron concentration level of $2 \times 10^{18}\,cm^{-3}$. $Al_{0.7}Ga_{0.3}N$ epilayers were grown at three different pyrometer temperatures, 1060 °C, 1120 °C, and 1160 °C with respective V/III ratios of 1800, 1700, and 1400. The reduction of V/III ratio with higher T_g is a consequence of an increased gas-phase Ga molar flux necessary to maintain a constant Ga film composition. As expected, a reduction in hillock size and smoother surfaces were observed for n-$Al_{0.7}Ga_{0.3}N$:Si films grown at 1160 °C compared to 1060 °C. However, both the electron concentration and electron mobility (μ) measured by Hall effect decreased with increased T_g. Table I summarizes these results. A higher n in the film grown at 1160 °C was not achieved by adjusting the Si molar flux. While improving surface morphology with higher T_g is desirable, reductions of n and μ are problematic and were investigated further.

Schottky diodes were formed from films grown at the end point temperatures of 1060 °C and 1160 °C to conduct further electrical and deep level defect characterization to understand this strong dependence of n and μ on T_g. Semi-transparent 80 Å Ni Schottky contacts were deposited on the n-$Al_{0.7}Ga_{0.3}N$ films, and ohmic contacts were established using indium. Capacitance-voltage (CV) measurements were performed to measure ionized donor concentration (N_d) less the compensating defect density ($N_d - N_t$) in the depletion region. CV sweeps were conducted at 10 kHz to avoid problems with series resistance in the heavily compensated film. The validity of the measured capacitance was confirmed by a phase angle that remained near −90° for all bias values. Table I shows the values for ($N_d - N_t$) that were determined from CV, and these agreed with the respective n values measure by Hall effect. These data verified that, rather than becoming a deep donor, Si dopants remained shallow at higher T_g. The much lower n for the film grown at higher T_g therefore resulted from heavy compensation due to excess point defect formation. Increasing point defect concentrations also explain the reduction in μ.

TABLE I. Summary of electronic properties of films as a function of T_g.

T_g (°C)	μ (cm^2/V/s)	n (cm^{-3})	($N_d - N_t$) (cm^{-3})
1060	100	2.0×10^{18}	2.2×10^{18}
1120	71	1.1×10^{18}	-
1170	41	2.9×10^{17}	3.8×10^{17}

III. RESULTS AND DISCUSSION

A. Deep level defect characterization

DLOS was performed to understand the strong dependence of deep level incorporation on T_g in these films. DLOS measures the diode photocapacitance induced by monochromatic illumination with sub-band gap light. Photocapacitance results from a change in space-charge following photoemission of a carrier from a deep level defect located in the depletion region. The optical signature of the deep level the optical cross-section (σ^0) is defined as the optical emission rate at a given photon energy ($h\nu$) normalized to the incident photon flux (ϕ), which can be thought of physically as the optical absorbance of the deep level per unit defect. Spectral variation of σ^0 is measured from the time derivative of the photocapacitance transient at the onset of illumination divided by ϕ. Details of DLOS have been described previously in the literature.[13] DLOS measurements were performed at 297 K and −6 V using a Xe arc lamp source filtered through a 1/4 meter monochromator with mode-sorting filters. A 0 V electrical fill pulse was applied after illumination at each $h\nu$ to re-populate defects, followed by a 30 s relaxation time to allow thermal transients to saturate. Similar to CV measurements, photocapacitance transients were recorded at 10 kHz using a lock-in amplifier and digitized using an oscilloscope.

Figure 1 shows the DLOS spectra of the n-$Al_{0.7}Ga_{0.3}N$ films grown at 1060 °C and 1160 °C. Bandedge absorption causes a saturation in both DLOS spectra at $h\nu = E_g = 4.95$ eV. Thresholds in the DLOS data in the $T_g = 1160$ °C film at sub-gap $h\nu$ near 1.8 eV, 3.1 eV, and 4.7 eV arise from optical absorption by deep level defects. These deep level spectra were fit simultaneously using the model of Pässler[14] for phonon-assisted defect absorption to determine the optical ionization energy (E_o) and the Franck-Condon energy (d_{FC}) of the defect levels by performing a non-linear least-squares fit to σ^o.

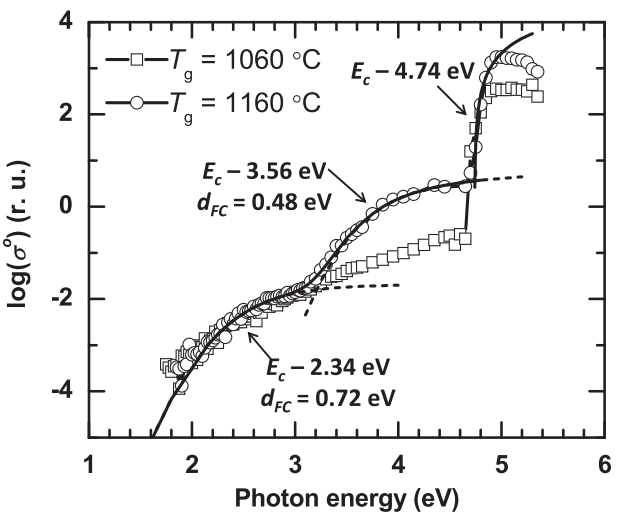

FIG. 1. DLOS spectra showing the evolution of deep level defects with T_g. The solid line between 1.6 and 4.6 eV is a simultaneous fit to the $E_c - 3.56$ eV and $E_c - 2.34$ eV deep levels, and the dotted lines show the individual σ^o spectra. The poorly resolved spectra for the $E_c - 3.56$ eV level in the $T_g = 1060$ °C film is due to a low signal-to-noise ratio and is a qualitative indication of reduced defect density compared to the film grown at $T_g = 1160$ °C.

TABLE II. Summary of deep level properties for films grown at 1060 °C and 1160 °C.

T_g (°C)	E_o (eV)	d_{FC} (eV)	N_t (cm^{-3})
1160	$E_c - 2.34$	0.72	1×10^{16}
1160	$E_c - 3.56$	0.48	5.1×10^{17}
1160	$E_c - 4.74$	0	6.6×10^{17}
1060	$E_c - 2.34$	0.72	2.2×10^{16}
1060	$E_c - 3.56$	0.48	4.1×10^{16}
1060	$E_c - 4.74$	0	1.0×10^{17}

Uncertainties for E_o and d_{FC} determined from the model of Pässler are ~ 0.05 eV. All changes in photocapacitance (ΔC) were positive, indicating majority carrier (electron) photoemission, so E_o values are referenced to the conduction band minimum (E_c). The fitted E_o and d_{FC} values are summarized in Table II. Photoemission occurred for $h\nu < E_o$ for the $E_c - 2.34$ eV and $E_c - 3.56$ eV deep levels due to phonon-assisted optical absorption operative for defect centers with strong lattice coupling.[14] The optical line-shape of the $E_c - 4.74$ eV deep level spectrum was very sharp with no evidence of phonon broadening ($d_{FC} = 0$ eV), consistent with an effective mass-like state.

DLOS corresponding to the $T_g = 1060$ °C film exhibited very similar deep level spectra, except that the $E_c - 3.56$ eV deep level was not well resolved. Nonetheless, it is likely that $E_c - 3.56$ eV deep level defect exists in the $T_g = 1060$ °C film. The experimental DLOS spectrum continues to show structure for $h\nu > 3.00$ eV, whereas the theoretical fit to the $E_c - 2.34$ eV alone (dashed line in Figure 1) predicts a flat DLOS spectrum in the absence of another defect level that is deeper in energy relative to E_c. The weaker signal-to-noise ratio for DLOS measurement of the $E_c - 3.56$ eV for the $T_g = 1060$ °C film could result from the much larger net doping, a lower deep level defect density, or both. Determination of N_t for all levels is discussed below, but their microscopic origins are considered next.

Possible physical origins of the three observed deep levels can be considered from comparison to previous studies of GaN and AlGaN. Firstly, the $E_c - 4.74$ eV deep level reported here has a sharp spectrum and energetic location ($E_v + 0.21$ eV) that are similar to a defect level that is commonly observed in *n*-type GaN at $E_c - 3.28$ eV, i.e., 0.16 eV above the valence band maximum (E_v), that has been attributed to either C or residual Mg impurities.[15,16] The similarity between the $E_c - 4.74$ eV $Al_{0.7}Ga_{0.3}N$ and $E_c - 3.28$ eV GaN defect states would suggest that they share a similar physical origin. However, secondary ion mass spectroscopy (SIMS) analysis of $Al_{0.7}Ga_{0.3}N$:Si films grown in the same reactor under similar growth conditions and T_g range show the C contamination level to be less than 5×10^{16} cm^{-3} and Mg contamination below the detection limit $< 1 \times 10^{16}$ cm^{-3}. These impurity concentrations are much lower than the concentration of the $E_c - 4.74$ eV defect state in either film studied here (determination of the deep level density is discussed below). These observations indicate that the $E_c - 4.74$ eV level originates from an as yet unidentified point defect source other than C of Mg. Secondly, association of the $E_c - 3.56$ eV deep level with the group-III vacancy (V_{III}) or related V_{III}-impurity complex is supported by comparing its DLOS spectrum with previous photoluminescence (PL), and positron annihilation spectroscopy (PAS) studies of $Al_xGa_{1-x}N$ (Refs. 17 and 18) and density functional theory (DFT) calculations of defect-related optical absorption and emission in AlN.[19] Within the one-dimensional configuration-coordinate model,[19] a PL band that derives from the $E_c - 3.56$ eV deep level is expected have a very broad spectrum with peak energy at approximately $E_o - 2d_{FC} = 2.6$ eV. This value agrees well with the trend of PL peak energies versus x for a broad deep level PL band tracked across the entire $Al_xGa_{1-x}N$ alloy range that was ascribed to V_{III} (2-/3-) charge states.[17] Broad PL peaks near 2.6 eV were also observed in $Al_{0.6}Ga_{0.4}N$:Si and conclusively associated with V_{III}–related defects by correlating the increase in integrated PL intensity with increasing PAS *S*-parameter, i.e., increasing V_{III}–related defect concentration, as a function of Si concentration $> 1 \times 10^{18}$ cm^{-3}.[18] The E_o and d_{FC} values obtained for the $E_c - 3.56$ eV deep level are also in reasonable agreement for corresponding values calculated for the V_{Al} (3-/2-) optical transition in AlN,[19] which is likely to be similar to V_{III}-related transitions in $Al_{0.7}Ga_{0.3}N$ Finally, the atomistic origin of the $E_c - 2.34$ eV deep level defect remains a question for additional study as it does not appear to have an analog from previous defect studies of $Al_xGa_{1-x}N$.

B. Deep level defect density measurement

Measuring the concentration of the observed deep level defects is necessary to understand their role in the strong T_g dependence of Si dopant compensation. Table II lists measured values for N_t, which were determined in the following manners. Deep level defect concentration is often measured from the steady-state photocapacitance (SSPC). Figure 2 shows the relative SSPC, $\Delta C/C_0$, where C_0 is the dark capacitance, for both samples. The usual relationship $N_t \approx 2N_d \Delta C/C_0$ is valid only when $\Delta C/C_0 \ll 1$, i.e., $N_t \ll N_d$. This condition holds for the film growth at 1060 °C but is violated for the $E_c - 3.56$ eV and $E_c - 4.74$ eV deep levels in the $T_g = 1160$ °C film. Therefore, LCV was used to quantify N_t

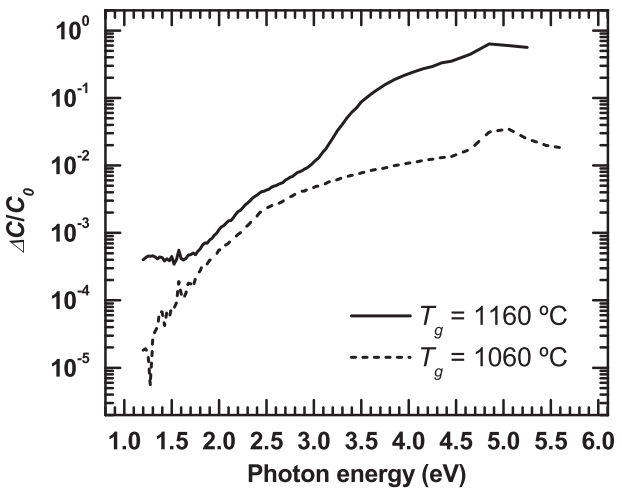

FIG. 2. Steady-state photocapacitance spectra for the AlGaN films. Note that $\Delta C/C_0 \approx 1$ for the $E_c - 3.56$ eV and $E_c - 4.74$ eV levels in the film grown at $T_g = 1160$ °C and therefore does not approximate N_t.

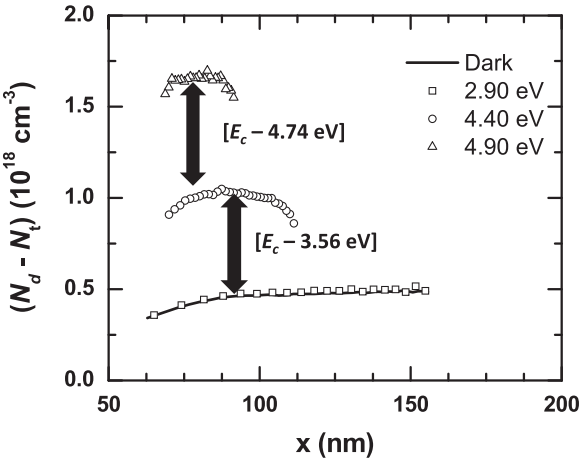

FIG. 3. Lighted capacitance-voltage scans for the film grown at $T_g = 1160\,^{\circ}$C. The large change in $(N_d - N_t)$ is approximately equal to N_t.

for these deep levels. LCV measures *CV* sweeps under sub-bandgap monochromatic illumination with $h\nu$ values chosen to empty deep levels one at a time.[20] For example, $[E_c - 3.56$ eV] (brackets denote defect concentration) for $T_g = 1160\,^{\circ}$C film is the difference in $(N_d - N_t)$ measured by *CV* at $h\nu = 2.90$ eV (with the defect fully occupied) and at $h\nu = 4.40$ eV (with the defect depopulated), as shown in Fig. 3. Likewise $[E_c - 4.74$ eV] was determined from the increase in space-charge density for $h\nu = 4.90$ eV relative to $h\nu = 4.40$ eV illumination.

IV. CONCLUSIONS

The source of significant dopant compensation with higher T_g can now be understood in terms of defect incorporation using the DLOS and LCV data. The $E_c - 3.54$ eV and $E_c - 4.74$ levels are identified as the major compensators for the $T_g = 1160\,^{\circ}$C $Al_{0.7}Ga_{0.3}N$ film owing to their large N_t. Indeed, when these deep levels are optically depopulated, the effective net doping concentration for the film grown at $T_g = 1160\,^{\circ}$C more than triples and becomes comparable to that for $T_g = 1060\,^{\circ}$C $Al_{0.7}Ga_{0.3}N$. As discussed previously, high T_g for Al-rich AlGaN can drive increased V_{III} concentration, which further supports attribution of the $E_c - 3.54$ eV level as being V_{III}-related. Kinetically driven excess Ga desorption at elevated T_g is anticipated and might not be fully compensated by increased Ga flow rates. Additionally, thermodynamics can drive acceptor-like deep level defect formation in *n*-type semiconductors with very large E_g.[9] The defect formation energy of an occupied versus charge-neutral deep acceptor defect in an *n*-type UWBG semiconductor is reduced by approximately $(E^{o} - d_{FC})$, which is of order E_g. In the case of a multiply charged defect center, such as V_{III}-related defects in *n*-type $Al_xGa_{1-x}N$, E^f is decreased substantially per captured carrier and can approach zero. Indeed, DFT calculations find E^f of V_{Al}^{3-} to become negative for *n*-type AlN,[21] leading to spontaneous vacancy formation. This trend suggests that an Al-rich AlGaN:Si crystal will naturally favor V_{III} formation when epitaxial growth conditions approach thermal equilibrium, such as with high T_g.

The increase in $[E_c - 4.74$ eV] with increasing T_g could also be thermodynamically driven. The sensitivity of E^f on Fermi level position is strongest for defect centers that form close to the minority carrier band edge (E_v in this case). The incorporation of acceptor-like impurities forming electronic states near E_v in Al-rich AlGaN:Si could become favorable with increasing T_g because E^f of the occupied deep acceptor would be reduced relative to the charge neutral state by approximately E_g, which approaches 6.2 eV for Al-rich AlGaN.

In summary, the dependence of Si doping efficiency and deep level defect formation was investigated for *n*-type $Al_{0.7}Ga_{0.3}N$ as a function of T_g. It was observed that dopant compensation by deep level defects was greatly reduced by lowering T_g. DLOS and LCV were employed to identify the major compensators as the $E_c - 3.56$ eV and $E_c - 4.74$ eV deep levels. The $E_c - 3.56$ eV defect level was attributed to V_{III} or related complex. The atomistic origin of the $E_c - 4.74$ eV level is unclear, but SIMS data conclusively ruled out C and Mg impurities. This finding suggests that physical source of near-valence band defect states in AlGaN changes with alloying since C and Mg are thought to be the primary source of near-valence band defect states in GaN and low Al mole fraction AlGaN.[15,16] Possible mechanisms for the strong T_g dependence of these defects were considered in terms of both growth kinetics and also thermodynamic processes driven by the large $Al_{0.7}Ga_{0.3}N$ band gap energy.

ACKNOWLEDGMENTS

This work was supported by Sandia National Laboratories Laboratory Directed Research and Development program. Sandia National Laboratories is a multi-program laboratory managed and operated by Sandia Corporation, a wholly owned subsidiary of Lockheed Martin Corporation, for the United States Department of Energy's National Nuclear Security Administration under Contract No. DE-AC04-94AL85000.

[1]H. Hahn, B. Reuters, H. Kalisch, and A. Vescan, Semicond. Sci. Technol. **28**, 074017 (2013).
[2]J. Xie, S. Mia, R. Dalmau, R. Collazo, A. Rice, J. Tweedie, and Z. Sitar, Phys. Status Solidi C **8**, 2407 (2011).
[3]S. Hashimoto, K. Akita, Y. Yamamoto, M. Ueno, T. Nakamura, K. Takeda, M. Iwaya, Y. Honda, and H. Amano, Phys. Status Solidi A **209**, 501 (2012).
[4]H. Tokuda, M. Hatano, N. Yafune, S. Hashimoto, K. Akita, Y. Yamamoto, and M. Kuzuhara, Appl. Phys. Express **3**, 121003 (2010).
[5]S. Hashimoto, K. Akita, Y. Yamamoto, M. Ueno, T. Nakamura, N. Yafune, K. Sakuno, H. Tokuda, M. Kuzuhara, K. Takeda, M. Iwaya, and H. Amano, Phys. Status Solidi C **9**, 373 (2012).
[6]J. L. Hudgins, G. S. Simin, E. Santi, and M. A. Khan, IEEE Trans. Power Electron. **18**, 907 (2003).
[7]A. Q. Huang, IEEE Electron Device Lett. **25**, 298 (2004).
[8]J.-Y. Duboz, N. Grandjean, F. Omnes, M. Mosca, and J.-L. Reverchon, Appl. Phys. Lett. **86**, 063511 (2005).
[9]W. Walukiewicz, Phys. B Condens. Matter **302**, 123 (2001).
[10]F. Mehnke, T. Wernicke, H. Pingel, C. Kuhn, C. Reich, V. Kueller, A. Knauer, M. Lapeyrade, M. Weyers, and M. Kneissl, Appl. Phys. Lett. **103**, 212109 (2013).
[11]R. Collazo, S. Mita, J. Xie, A. Rice, J. Tweedie, R. Dalmau, and Z. Sitar, Phys. Status Solidi C **8**, 2031 (2011).
[12]A. Kakanakova-Georgieva, D. Nilsson, X. T. Trinh, U. Forsberg, N. T. Son, and E. Janzén, Appl. Phys. Lett. **102**, 132113 (2013).

[13]A. Chantre, G. Vincent, and D. Bois, Phys. Rev. B **23**, 5335 (1981).
[14]R. Paüssler, J. Appl. Phys. **96**, 715 (2004).
[15]A. Armstrong, A. R. Arehart, D. Green, U. K. Mishra, J. S. Speck, and S. A. Ringel, J. Appl. Phys. **98**, 053704 (2005).
[16]A. Hierro, D. Kwon, S. A. Ringel, M. Hansen, J. S. Speck, U. K. Mishra, and S. P. DenBaars, Appl. Phys. Lett. **76**, 3064 (2000).
[17]K. B. Nam, M. L. Nakarmi, J. Y. Lin, and H. X. Jiang, Appl. Phys. Lett. **86**, 222108 (2005).
[18]S. F. Chichibu, H. Miyake, Y. Ishikawa, M. Tashiro, T. Ohtomo, K. Furusawa, K. Hazu, K. Hiramatsu, and A. Uedono, J. Appl. Phys. **113**, 213506 (2013).
[19]Q. Yan, A. Janotti, M. Scheffler, and C. G. V. de Walle, Appl. Phys. Lett. **105**, 111104 (2014).
[20]A. Armstrong, A. R. Arehart, and S. A. Ringel, J. Appl. Phys. **97**, 083529 (2005).
[21]C. Stampfl and C. Van de Walle, Phys. Rev. B **65**, 155212 (2002).